PHYSICAL REVIEW A **90**, 013423 (2014)

Attosecond streaking of Cohen-Fano interferences in the photoionization of H_2^+

Qi-Cheng Ning,[1] Liang-You Peng,[1,2,*] Shu-Na Song,[1] Wei-Chao Jiang,[1] Stefan Nagele,[3,†] Renate Pazourek,[3]
Joachim Burgdörfer,[3] and Qihuang Gong[1,2]
[1]*State Key Laboratory for Mesoscopic Physics and Department of Physics, Peking University, Beijing 100871, China*
[2]*Collaborative Innovation Center of Quantum Matter, Beijing 100871, China*
[3]*Institute for Theoretical Physics, Vienna University of Technology, 1040 Vienna, Austria, EU*

(Received 23 January 2014; published 30 July 2014)

We present a numerical *ab-initio* simulation of the time delay in the photoionization of the simplest diatomic molecule H_2^+ as observed by attosecond streaking. We show that the strong variation of the Eisenbud-Wigner-Smith time delay t_{EWS} as a function of energy and emission angle becomes observable in the streaking time shift t_{S} provided laser field induced components are accounted for. The strongly enhanced photoemission time shifts are traced to destructive Cohen-Fano (or two-center) interferences. Signatures of these interferences in the streaking trace are shown to be enhanced when the ionic fragments are detected in coincidence.

DOI: 10.1103/PhysRevA.90.013423 PACS number(s): 32.80.Rm, 31.15.A−, 42.50.Hz, 42.65.Re

I. INTRODUCTION

Since the very first experimental demonstration of attosecond pulses and pulse trains [1,2], these new light sources, synchronized with an infrared (IR) laser pulse, have enabled the probe and control of the electronic dynamics inside atoms and molecules on its natural time scale (see, e.g., [3,4] and references therein). In particular, the attosecond streak camera [5–9] and interferometric approaches including the RABBITT (reconstruction of attosecond beating by interference of two-photon transitions) technique [10–16] have been developed into powerful tools to access the quantum phase information and phase variation in atomic and molecular ionization. With these advances, attosecond physics now allows one to address fundamental quantum-mechanical issues in the time domain, in particular, how long it takes for an electron to escape from the atomic core or a solid surface following absorption of a photon [17].

First proof-of-principle experimental demonstrations include measurements of time delayed photoemission from the core levels relative to conduction band states of a tungsten surface [6] and, more recently, a time delay of 21 ± 5 as between photoemission from $2p$ and $2s$ subshells of atomic neon [7]. These observations have triggered a large number of theoretical investigations of the time delay in atomic photoionization [18–37], molecular photoionization [37–39], and photoemission from surfaces [40–42]. For example, the methods employed to describe the photoionization process in neon include the state-specific expansion approach [7], the random-phase approximation with exchange (RPAE) [19,26], diagrammatic many-body perturbation theory [28], the time-dependent R-matrix method [36], and the B-spline R-matrix method [43], none of which, however, have up to now been able to account for the experimentally observed delay. Similarly, the difference in photoionization time delays between electrons emitted from $3s^2$ and $3p^6$ shells of Ar were measured with the RABBITT technique [15,16] and yield for photon energies close to the Cooper minimum [44,45] sizable discrepancies to calculations using the RPAE method [16,26], the multiconfigurational Hartree-Fock close-coupling ansatz [30], or the time-dependent local-density approximation [37]. The origin of these discrepancies for such a fundamental property of atomic photoemission remains a widely open question with so far unaccounted multielectron correlations being one of the prime suspects. Indeed, recent *ab initio* simulations on one-electron attosecond streaking of He with the shakeup of the second electron clearly demonstrate the significant contribution of electron-electron correlation to the photoionization time delays [22].

Time-resolved photoionization of more complex systems with internal geometric structure promises novel insights into the formation of an outgoing wave packet emerging from the complex. The simplest prototypical case is the photoionization of a diatomic molecule [38,46–48]. The fundamental questions to be addressed include the following: does it take a longer time for the electron to escape from the multicenter molecular core than from the one-center atomic core?; does the emission time delay dependence on the energy and on the relative orientation of the emission direction and molecular axis carry information on the geometric arrangement of the atomic constituents?; and, most importantly, are those effects observable in an attosecond streaking setting? We present in the following an *ab initio* simulation of the attosecond streaking time delay t_{S} and the extraction of the intrinsic Eisenbud-Wigner-Smith (EWS) time delay t_{EWS} [49–51] for H_2^+ ionized by an extreme ultraviolet (XUV) pulse and probed by a few-cycle infrared (IR) field. We show that the Cohen-Fano (or two-center) interferences [52–54] leave a clear and observable mark on the streaking time delay. Destructive path interferences suppress the formation of the electronic wave packet and greatly increase the magnitude of the EWS time delay, which can be either positive (delay) or negative (advance).

II. EWS DELAYS AND SIMULATION OF ATTOSECOND STREAKING

In our numerical attosecond streaking simulation, the time-dependent electronic Schrödinger equation (TDSE) of

---

[*] liangyou.peng@pku.edu.cn
[†] stefan.nagele@tuwien.ac.at

H_2^+ in the presence of the ionizing XUV attosecond pulse and the probing IR streaking field is accurately solved in prolate spheroidal coordinates. The momentum spectrum of the ionized electron is extracted by projecting the wave packet after the end of the laser pulses onto the molecular scattering states ψ_f^- with incoming wave boundary conditions (see [55] and references therein for details). The photoionization is calculated at fixed internuclear distance R and fixed orientation of the internuclear axis as a vertical Franck-Condon-like electronic transition between Born-Oppenheimer (BO) potential surfaces. This approximation is well justified for ultrashort attosecond XUV pulses. We present results for fixed internuclear distance and alignment angle of the H_2^+ molecules, as well as calculations where the distribution of R in the vibronic ground state and the distribution of the alignment angle of laser-aligned molecules are taken into account through an ensemble average over Franck-Condon transitions. For comparison, also simulations for atomic targets are performed within the single-active-electron (SAE) approximation [56,57]. All results were checked for convergence by variation of the temporal and spatial parameters in the TDSE simulations.

The XUV pulses of mean frequency ω_{XUV} employed in the streaking simulations have a Gaussian envelope with a full width at half maximum (FWHM) duration ranging from $\tau_{\mathrm{XUV}} = 400$ to 600 as and a peak intensity of $I_{\mathrm{XUV}} = 10^{12}$ W/cm^2. The angle between the linear polarization of the XUV pulse and the internuclear axis is denoted by θ_x. The comparatively long τ_{XUV} is chosen to reduce bandwidth effects which would obscure sharp spectral features. The streaking IR field has a total duration of two optical cycles at a wavelength of 800 nm with a cosine-squared envelope of the vector potential (i.e., the carrier envelope phase is zero). In order to minimize distortion effects of the initial states as well as rescattering effects [55,56] we consider weak IR streaking fields ranging in intensity I_{IR} from 10^8 to 10^{11} W/cm^2 and check for the independence of the extracted time information of I_{IR}. In the presence of the IR field, the final electron momentum $\vec{p}_f$ is related to the unperturbed asymptotic momentum $\vec{p}_0$ for a given delay τ between the XUV and IR pulses as $\vec{p}_f(\tau) = \vec{p}_0 - \vec{A}_{\mathrm{IR}}(\tau + t_{\mathrm{S}})$. The absolute streaking time delays t_{S} relative to the peak of the XUV pulse are extracted by fitting the first moment of the electron momentum spectra along $\theta_e = 0^\circ$ (or $\theta_e = \pi$), where θ_e is the electron ejection angle relative to the internuclear axis, to the IR vector potential $\vec{A}_{\mathrm{IR}}$ [Fig. 1(a)]. The relative shift between the two sinusoidal curves is the only fitting parameter and determines t_{S} [20].

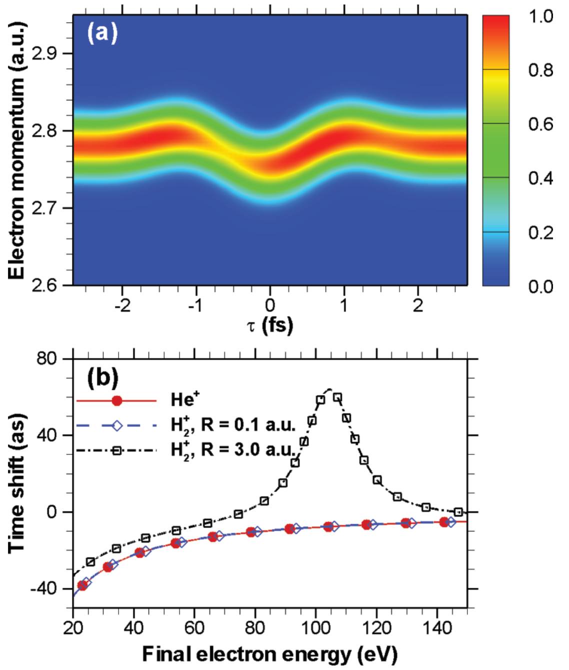

FIG. 1. (Color online) (a) Typical streaking spectrogram for ionization of H_2^+ by a 130-eV XUV pulse [$\theta_x = 0^\circ$, $\tau_{\mathrm{XUV}} = 400$ as (FWHM)] probed by a 800-nm two-cycle streaking field with intensity $I_{\mathrm{IR}} = 10^{11}$ W/cm^2 for electron emission along the polarization axis of the streaking field ($\theta_e = 0^\circ$) and fixed internuclear distance $R = 3$ a.u. (b) Extracted streaking delays t_{S} for He$^+$ (red circles), H_2^+ at $R = 0.1$ a.u. (blue diamonds), and H_2^+ at $R = 3.0$ a.u. (black squares) for pulse parameters $\tau_{\mathrm{XUV}} = 600$ as (FWHM) and $I_{\mathrm{IR}} = 10^8$ W/cm^2.

In the limit of small internuclear distance R [$R = 0.1$ a.u., Fig. 1(b)], the streaking delays of H_2^+ approach those of the united atom limit, $H_2^+ \rightarrow$ He$^+$, rendering molecular effects on the time delay entirely negligible. The agreement of our H_2^+ results in this limit with calculations for He$^+$ (cf. [20]) demonstrates the robustness and reliability of our numerical methods. At larger distances, e.g., $R = 3$ [Fig. 1(b)], a remarkably different picture emerges: the streaking delay is strongly enhanced with a broad maximum reaching values $t_{\mathrm{S}} \approx 64$ as. This signature of pronounced molecular structures in the streaking time delay can be traced to the behavior of the intrinsic EWS time delay, t_{EWS} (see Fig. 2). For atomic photoionization the additivity of the EWS delay, the IR field induced Coulomb-laser coupling (CLC), and dipole-laser coupling (dLC) delays

$$t_{\mathrm{S}} = t_{\mathrm{EWS}} + t_{\mathrm{CLC}} + t_{\mathrm{dLC}} \tag{1}$$

has been established (see [20,22,23] for a detailed discussion). Since the long-range Coulomb interaction (t_{CLC}) and dipole potentials are independent of short-ranged potentials, Eq. (1) is expected to hold for molecules as well (for nonpolar molecules $t_{\mathrm{dLC}} = 0$). The EWS time delay t_{EWS} for the H_2^+ molecule can

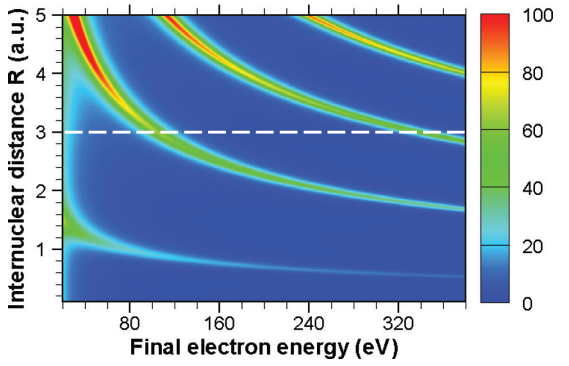

FIG. 2. (Color online) EWS delay t_{EWS} in the (E,R) plane for emission along the internuclear axis $\theta_e = 0^\circ$ and the XUV pulse polarized parallel to the internuclear axis, $\theta_x = 0^\circ$. The EWS delays that are contained in the streaking results of Fig. 1(b) [Eq. (1)] correspond to cuts for constant R (dashed line for $R = 3$).

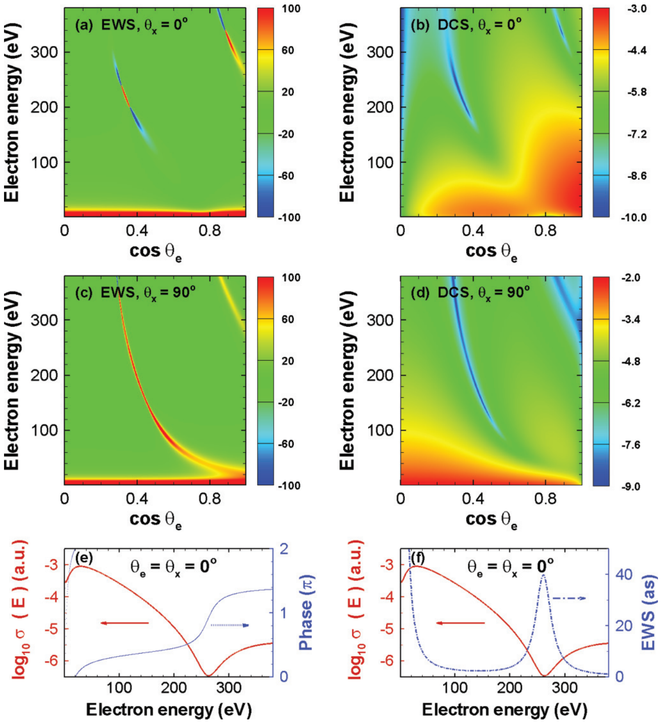

FIG. 3. (Color online) EWS time delays of H_2^+ at the equilibrium distance $R = 2$ a.u., plotted as a function of electron energy E and ejection angle θ_e [$t_{\mathrm{EWS}}(E,\theta_e)$] for the XUV pulse polarized (a) parallel ($\theta_x = 0^\circ$) or (c) perpendicular ($\theta_x = 90^\circ$) with respect to the molecular axis. The corresponding single-photon differential ionization cross sections (DCS) in (b) and (d) are plotted on a logarithmic scale. A cut of the DCS at $\theta_e = 0$ for the case $\theta_x = 0$ is plotted along with the phase of the transition matrix element in (e) and along with the EWS delay t_{EWS} in (f).

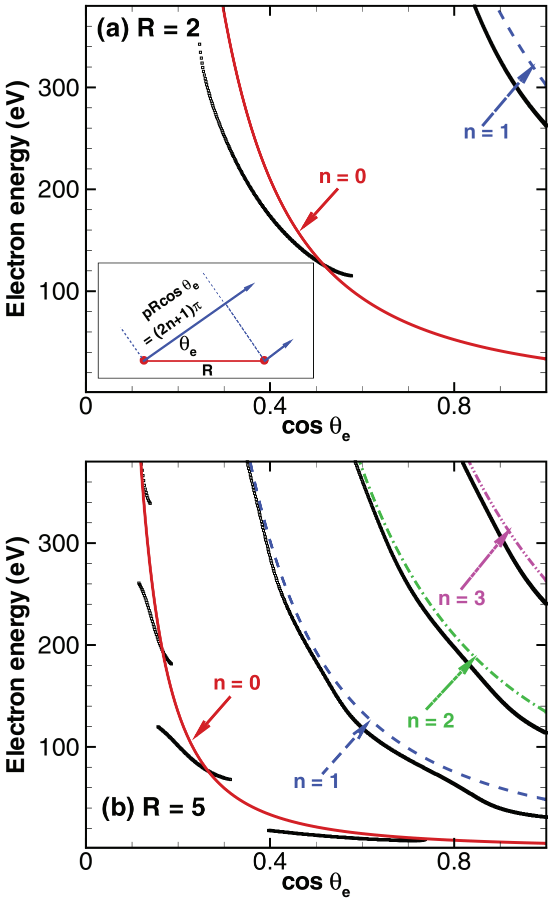

FIG. 4. (Color online) Comparison between the location of the minima in the differential photoionization cross section (DCS) in the $(E, \cos\theta_e)$ plane with the prediction of the two-center interference model according to $\sqrt{2E}R\cos\theta_e = (2n+1)\pi$ [see inset in (a)] for different n. The DCS is given for a Franck-Condon transition at (a) $R = 2$ and (b) $R = 5$. Note that the extraction of well-defined minima from the very small DCS is not always possible, giving rise to the discontinuities.

be calculated (separately from the TDSE solution) from the energy derivative of the phase of the exact dipole transition element in the absence of a streaking field:

$$t_{\mathrm{EWS}}(E,R,\theta_e,\theta_x) = \frac{\partial}{\partial E}\arg(\langle\psi_f^-(E,R,\theta_e)|\vec{d}\cdot\hat{e}|\phi_0\rangle), \quad (2)$$

where E is the final continuum energy of the emitted electron, $|\phi_0\rangle$ is the molecular ground-state, $\vec{d}$ is the dipole operator, and $\hat{e}$ is the polarization axis of the XUV field.

The landscape of the EWS delay as a function of the internuclear distance R and the emission energy $E = \hbar\omega_{\mathrm{XUV}} - I_p$ (Fig. 2) reveals that the peak in t_S (Fig. 1) directly maps out the peak in the EWS time distribution. The residual difference between t_S and t_{EWS} (not shown) is given by the CLC delay t_{CLC} as predicted by Eq. (1), validating Eq. (1) also for molecules. In particular, the CLC contributions t_{CLC} for the ionization of the H_2^+ molecule and its isoelectric atomic partner He^+ [20] are identical.

The distribution of t_{EWS} in the θ_e-E plane (Fig. 3) for fixed internuclear distance shows that the ridges of enhanced delays are also directly linked to minima in the energy-differential and angle-differential cross sections (DCSs). The distribution is largely independent of the orientation of the polarization axis of the ionizing pulse, pointing to a continuum final-state effect. The minima in the DCS with the accompanying maxima in the EWS delays are reminiscent of the behavior of Cooper minima [44,45] characterized by a rapid phase jump by $\pm\pi$ of the transition matrix element [Fig. 3(e)]. In the present case, however, they allow for a simple intuitive description in terms of a semiclassical path interference. Cohen and Fano [52] pointed out that the energy and angular distribution of the photoelectrons from diatomic molecules feature two-center path interferences. Destructive interference between emission from the two centers occurs when the electron momentum $\vec{p}$ and the internuclear distance vector $\vec{R}$ satisfy $\vec{p}\cdot\vec{R} = pR\cos\theta_e = (2n+1)\pi$, valid in the limit of high electron energies when the outgoing waves can be approximated by plane waves (Fig. 2). The lines in the $\cos\theta_e$-E plane for which destructive interference $\sqrt{2E}R\cos\theta_e = (2n+1)\pi$ holds approximate the minima in the DCS and, in turn, the extrema in t_{EWS} quite well (Fig. 4), confirming two-center interferences as the origin of the enhanced EWS time shifts. Taking into account the phase distortion due to two-center

Coulomb effects within an eikonal approximation is expected to further improve the agreement. The destructive interference suppresses the emission of the outgoing wave packet and the magnitude of the corresponding t_{EWS} delay is significantly increased.

III. OBSERVABILITY OF THE TWO-CENTER EFFECT

It is now important to inquire into the observability of this two-center interference enhanced time delay in a realistic streaking setting accounting for the distribution of R in the vibronic ground state as well as the distribution of the alignment angle between the molecules and the probing fields. As the destructive interference is associated with a minimum in the cross section, visibility in the streaking signal is *a priori* not obvious. We parenthetically note that for the same reason also the enhanced time delay near Cooper minima is difficult to detect. We therefore include in our calculations corrections beyond the Franck-Condon transitions for photoemission from the molecule at the (fixed) equilibrium internuclear distance and beyond space-fixed orientation of the internuclear axis. The vibrational ground state of the H_2^+ molecule is described by a probability density $W_0(R)$ centered at the equilibrium distance $R_0 = 2$ a.u. We average the observable $O(R)$ calculated in the BO limit over an R-distribution $W(R)$ weighted by the corresponding ionization cross-section $\sigma(R)$:

$$\langle O \rangle_R = \frac{\int O(R)\, W(R)\, \sigma(R) dR}{\int W(R)\, \sigma(R) dR}. \qquad (3)$$

Specifically, the time shift $\langle t_{\mathrm{S}} \rangle_R$ is obtained as a weighted average over a large number of full streaking simulations for different R. Similarly, we take into account that for a laser-aligned molecule the molecular axis will have an angular distribution around the alignment axis for which we assume a Gaussian distribution with full width at half maximum of up to 15°. However, averaging over an alignment angle of 15° hardly changes the resulting EWS delays calculated from Eq. (2) and has thus negligible effects on the streaking delays [see Eq. (1)] since the CLC contribution is independent of the alignment angle.

The vibrational average over $W_0(R)$ fills in the deep minimum in the photoionization cross section caused by the two-center interference [Fig. 5(a)]. As a result, the prominent peak in the EWS delay disappears and is reduced to a very broad ridge on the 1- to 2-as level in $\langle t_{\mathrm{EWS}} \rangle_R$, and, in turn, in the averaged streaking delay $\langle t_{\mathrm{S}} \rangle_R$ [Fig. 5(b)]. The average over the entire vibrational ground-state distribution, thus, renders the change in time shift to be barely detectable.

Since photoionization of H_2^+ initiates the Coulomb explosion of the ionic fragments [58,59], however, energy resolved coincident detection of one outgoing proton allows to experimentally postselect a narrow R-distribution $W_\Delta(R)$ within the ground-state vibrational distribution. This additional "knob" allows to enhance the interference contrast in the time shifts by reducing the vibrational averaging. Coincident detection of a proton with an energy near the Coulomb explosion energy at the equilibrium distance, $E_{\mathrm{kin}} = 1/2R_0$, with an energy resolution (FWHM) of 0.5 eV selects a narrow radial distribution $W_\Delta(R)$ centered at R_0 with a width of $\Delta R = 0.15$ a.u. The reduced vibrational average, Eq. (3), now yields clearly visible peaks in the EWS and streaking time delays of the order of 10 as [Fig. 5(b)] as signatures of the destructive interference.

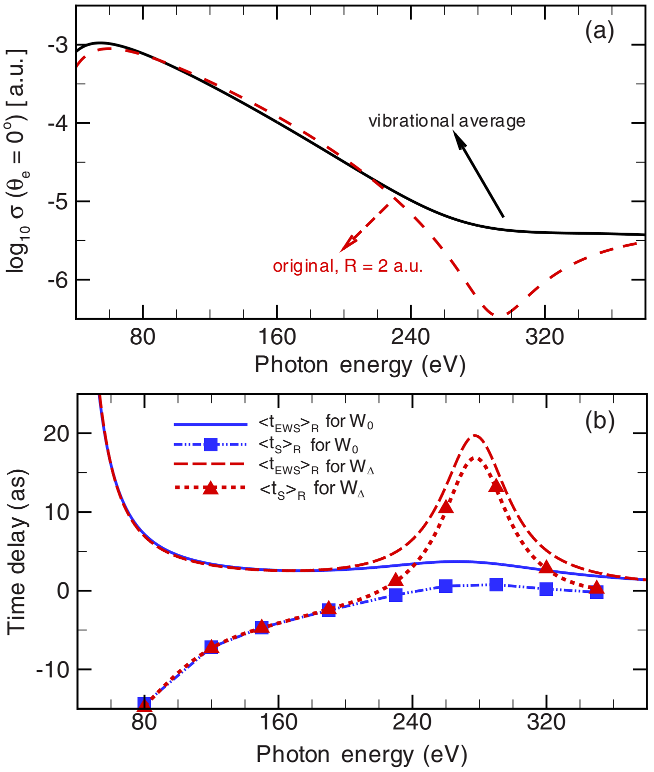

FIG. 5. (Color online) (a) Comparison between the differential cross section (DCS) at fixed internuclear equilibrium distance $R = 2$ and averaged over the vibrational ground-state distribution W_0. (b) Expectation values $\langle t_{\mathrm{EWS}} \rangle_R$ and $\langle t_{\mathrm{S}} \rangle_R$ after averaging over the vibrational ground-state distribution W_0 (squares) and the distribution W_Δ (triangles) postselected from the Coulomb explosion of the molecular fragments. The XUV pulse duration in the streaking simulations is $\tau_{\mathrm{XUV}} = 600$ as (FWHM) and the intensity of the probing 800-nm field is $I_{\mathrm{IR}} = 10^8$ W/cm^2.

In order to preclude any polarization effects due to a strong IR field which might play, unlike for streaking of a structureless electron spectrum [20], a more important role near zeros of the photoionization cross section, we have performed streaking simulations with intensities as low as 10^8 W/cm^2. Increasing the streaking intensity to a typical experimental value of 10^{11} W/cm^2, the streaking trace becomes forward-backward ($\theta_e = 0°$ relative to $\theta_e = 180°$) asymmetric and the extracted t_{S} differ from each other, indicating the influence of IR multiphoton interferences. Remarkably, the average over the forward-backward asymmetry, $[t_{\mathrm{S}}(\theta_e = 0°) + t_{\mathrm{S}}(\theta_e = 180°)]/2$, agrees very well with t_{S} extracted at low intensity, thereby canceling out IR polarization effects (or multiphoton interferences) and allowing for an intensity independent measurement of t_{S}. We are therefore confident that the predicted enhanced streaking delays due to two-center interferences are experimentally accessible.

IV. CONCLUSIONS

Summarizing, we have simulated the attosecond streaking of photoionization of the simplest molecule H_2^+ by solving the time-dependent Schrödinger equation in the presence of the ionizing XUV and streaking IR fields. Our calculations include the effects of the vibrational distribution and the distribution of the molecular alignment angle. We have shown that from the observable streaking delay the intrinsic Eisenbud-Wigner-Smith time delay can be unambiguously extracted. Formation of the wave packet of the ionized electron is significantly modified when the Cohen-Fano condition for destructive two-center interference is met. We have proposed a protocol for electron streaking in coincidence with the ionic fragment in order to suppress the effect of vibrational averaging. We hope the current study of H_2^+ will stimulate experiments on photoionization time delays of molecules.

ACKNOWLEDGMENTS

L.Y.P. appreciates useful discussions and suggestions of Lars Bojer Madsen at the initial stage of this work. This work is supported in part by National Natural Science Foundation of China under Grants No. 11322437, No. 11174016, and No. 11121091; by the 973 Program under Grant No. 2013CB922402; by the Program for New Century Excellent Talents in University; and by the Austrian Science Fund (FWF) SFB041 (VICOM) and SFB049 (NEXTLITE). The computational results presented have been achieved in part by using the computer cluster "MESO" in the State Key Laboratory for Mesoscopic Physics at Peking University, by using the Vienna Scientific Cluster, and through XSEDE resources provided under Grant No. TG-PHY090031.

[1] P. M. Paul, E. S. Toma, P. Breger, G. Mullot, F. Augé, Ph. Balcou, H. G. Muller, and P. Agostini, Science **292**, 1689 (2001).
[2] M. Hentschel, R. Kienberger, Ch. Spielmann, G. A. Reider, N. Milosevic, T. Brabec, P. Corkum, U. Heinzmann, M. Drescher, and F. Krausz, Nature (London) **414**, 509 (2001).
[3] M. F. Kling and M. J. J. Vrakking, Annu. Rev. Phys. Chem. **59**, 463 (2008).
[4] F. Krausz and M. Ivanov, Rev. Mod. Phys. **81**, 163 (2009).
[5] R. Kienberger *et al.*, Nature (London) **427**, 817 (2004).
[6] A. L. Cavalieri *et al.*, Nature (London) **449**, 1029 (2007).
[7] M. Schultze *et al.*, Science **328**, 1658 (2010).
[8] J. Itatani, F. Quéré, G. L. Yudin, M. Y. Ivanov, F. Krausz, and P. B. Corkum, Phys. Rev. Lett. **88**, 173903 (2002).
[9] M. Kitzler, N. Milosevic, A. Scrinzi, F. Krausz, and T. Brabec, Phys. Rev. Lett. **88**, 173904 (2002).
[10] K. J. Schafer, M. B. Gaarde, A. Heinrich, J. Biegert, and U. Keller, Phys. Rev. Lett. **92**, 023003 (2004).
[11] T. Remetter *et al.*, Nat. Phys. **2**, 323 (2006).
[12] M. Swoboda, T. Fordell, K. Klünder, J. M. Dahlström, M. Miranda, C. Buth, K. J. Schafer, J. Mauritsson, A. L'Huillier, and M. Gisselbrecht, Phys. Rev. Lett. **104**, 103003 (2010).
[13] P. Johnsson *et al.*, Phys. Rev. Lett. **95**, 013001 (2005).
[14] P. Johnsson, J. Mauritsson, T. Remetter, A. L'Huillier, and K. J. Schafer, Phys. Rev. Lett. **99**, 233001 (2007).
[15] K. Klünder *et al.*, Phys. Rev. Lett. **106**, 143002 (2011).
[16] D. Guénot *et al.*, Phys. Rev. A **85**, 053424 (2012).
[17] H. W. van der Hart, Science **328**, 1645 (2010).
[18] C. H. Zhang and U. Thumm, Phys. Rev. A **82**, 043405 (2010).
[19] A. S. Kheifets and I. A. Ivanov, Phys. Rev. Lett. **105**, 233002 (2010).
[20] S. Nagele, R. Pazourek, J. Feist, K. Doblhoff-Dier, C. Lemell, K. Tőkési, and J. Burgdörfer, J. Phys. B **44**, 081001 (2011).
[21] S. Nagele, R. Pazourek, J. Feist, and J. Burgdörfer, Phys. Rev. A **85**, 033401 (2012).
[22] R. Pazourek, J. Feist, S. Nagele, and J. Burgdörfer, Phys. Rev. Lett. **108**, 163001 (2012).
[23] R. Pazourek, S. Nagele, and Joachim Burgdörfer, Faraday Discuss. **163**, 353 (2013).
[24] J. C. Baggesen and L. B. Madsen, Phys. Rev. Lett. **104**, 043602 (2010).
[25] M. Ivanov and O. Smirnova, Phys. Rev. Lett. **107**, 213605 (2011).
[26] A. S. Kheifets, Phys. Rev. A **87**, 063404 (2013).
[27] J. M. Dahlström, A. L'Huillier, and A. Maquet, J. Phys. B **45**, 183001 (2012).
[28] J. M. Dahlström, T. Carette, and E. Lindroth, Phys. Rev. A **86**, 061402(R) (2012).
[29] J. M. Dahlström, D. Guénot, K. Klünder, M. Gisselbrecht, J. Mauritsson, A. L'Huillier, A. Maquet, and R. Taïeb, Chem. Phys. **414**, 53 (2013).
[30] T. Carette, J. M. Dahlström, L. Argenti, and E. Lindroth, Phys. Rev. A **87**, 023420 (2013).
[31] M. D. Śpiewanowski and L. B. Madsen, Phys. Rev. A **86**, 045401 (2012).
[32] J. Su, H. Ni, A. Becker, and A. Jaroń-Becker, Phys. Rev. A **87**, 033420 (2013).
[33] J. Su, H. Ni, A. Becker, and A. Jaroń-Becker, J. Mod. Opt. **60**, 1484 (2013).
[34] J. Su, H. Ni, A. Becker, and A. Jaroń-Becker, Phys. Rev. A **88**, 023413 (2013).
[35] I. A. Ivanov and A. S. Kheifets, Phys. Rev. A **87**, 033407 (2013).
[36] L. R. Moore, M. A. Lysaght, J. S. Parker, H. W. van der Hart, and K. T. Taylor, Phys. Rev. A **84**, 061404(R) (2011).
[37] G. Dixit, H. S. Chakraborty, and M. El-Amine Madjet, Phys. Rev. Lett. **111**, 203003 (2013).
[38] V. V. Serov, V. L. Derbov, and T. A. Sergeeva, Phys. Rev. A **87**, 063414 (2013).
[39] I. A. Ivanov, A. S. Kheifets, and V. V. Serov, Phys. Rev. A **86**, 063422 (2012).
[40] A. K. Kazansky and P. M. Echenique, Phys. Rev. Lett. **102**, 177401 (2009).
[41] C. H. Zhang and U. Thumm, Phys. Rev. Lett. **102**, 123601 (2009).
[42] C. Lemell, B. Solleder, K. Tőkési, and J. Burgdörfer, Phys. Rev. A **79**, 062901 (2009).
[43] J. Feist, O. Zatsarinny, S. Nagele, R. Pazourek, J. Burgdörfer, X. Guan, K. Bartschat, and B. I. Schneider, Phys. Rev. A **89**, 033417 (2014).
[44] J. W. Cooper, Phys. Rev. **128**, 681 (1962).
[45] U. Fano and J. W. Cooper, Rev. Mod. Phys. **40**, 441 (1968).
[46] J. Fernández, O. Fojón, A. Palacios, and F. Martín, Phys. Rev. Lett. **98**, 043005 (2007).
[47] S. Haessler *et al.*, Phys. Rev. A **80**, 011404(R) (2009).
[48] J. Caillat, A. Maquet, S. Haessler, B. Fabre, T. Ruchon, P. Salières, Y. Mairesse, and R. Taïeb, Phys. Rev. Lett. **106**, 093002 (2011).

[49] L. Eisenbud, Ph.D. thesis, Princeton University, 1948.
[50] E. P. Wigner, Phys. Rev. **98**, 145 (1955).
[51] F. T. Smith, Phys. Rev. **118**, 349 (1960).
[52] H. D. Cohen and U. Fano, Phys. Rev. **150**, 30 (1966).
[53] T. Zuo and A. D. Bandrauk, Phys. Rev. A **52**, R2511 (1995).
[54] S. X. Hu, L. A. Collins, and B. I. Schneider, Phys. Rev. A **80**, 023426 (2009).
[55] X. F. Hou, L. Y. Peng, Q. C. Ning, and Q. Gong, J. Phys. B **45**, 074019 (2012).
[56] M. H. Xu, L. Y. Peng, Z. Zhang, Q. Gong, X. M. Tong, E. A. Pronin, and A. F. Starace, Phys. Rev. Lett. **107**, 183001 (2011).
[57] M. V. Frolov, D. V. Knyazeva, N. L. Manakov, A. M. Popov, O. V. Tikhonova, E. A. Volkova, M. H. Xu, L. Y. Peng, L. W. Pi, and A. F. Starace, Phys. Rev. Lett. **108**, 213002 (2012).
[58] L. J. Frasinski, K. Codling, P. Hatherly, J. Barr, I. N. Ross, and W. T. Toner, Phys. Rev. Lett. **58**, 2424 (1987).
[59] S. Chelkowski, T. Zuo, O. Atabek, and A. D. Bandrauk, Phys. Rev. A **52**, 2977 (1995).